Langmuir

Article

pubs.acs.org/Langmuir

Temperature-Dependent Adsorption and Adsorption Hysteresis of a Thermoresponsive Diblock Copolymer

Junxue An,[†] Andra Dėdinaitė,[†,‡] Francoise M. Winnik,[§,∥] Xing-Ping Qiu,[§] and Per M. Claesson*[,†,‡]

[†]School of Chemical Science and Engineering, Department of Chemistry, Division of Surface and Corrosion Science, KTH Royal Institute of Technology, Drottning Kristinas väg 51, SE-100 44 Stockholm, Sweden

[‡]Chemistry, Materials and Surfaces, SP Technical Research Institute of Sweden, Box 5607, SE-114 86 Stockholm, Sweden

[§]Department of Chemistry and Faculty of Pharmacy, University of Montreal, CP 6128 Succursale Centre Ville, Montreal QC H3C3J7, Canada

[∥]WPI International Center for Materials Nanoarchitectonics (MANA), National Institute for Materials Science, 1-1 Namiki, Tsukuba, Ibaraki 305-0044 Japan

Supporting Information

ABSTRACT: A nonionic-cationic diblock copolymer, poly(2-isopropyl-2-oxazoline)$_{60}$-*b*-poly((3-acrylamidopropyl)-trimethylammonium chloride)$_{17}$, (PIPOZ$_{60}$-*b*-PAMPTMA$_{17}$), was utilized to electrostatically tether temperature-responsive PIPOZ chains to silica surfaces by physisorption. The effects of polymer concentration, pH, and temperature on adsorption were investigated using quartz crystal microbalance with dissipation monitoring and ellipsometry. The combination of these two techniques allows thorough characterization of the adsorbed layer in terms of surface excess, thickness, and water content. The high affinity of the cationic PAMPTMA$_{17}$ block to the negatively charged silica surface gives rise to a high affinity adsorption isotherm, leading to (nearly) irreversible adsorption with respect to dilution. An increase in solution pH lowers the affinity of PIPOZ to silica but enhances the adsorption of the cationic block due to increasing silica surface charge density, which leads to higher adsorption of the cationic diblock copolymer. Higher surface excess is also achieved at higher temperatures due to the worsening of the solvent quality of water for the PIPOZ block. Interestingly, a large hysteresis in adsorbed mass and other layer properties was observed when the temperature was cycled from 25 to 45 °C and then back to 25 °C. Possible causes for this temperature hysteresis are discussed.

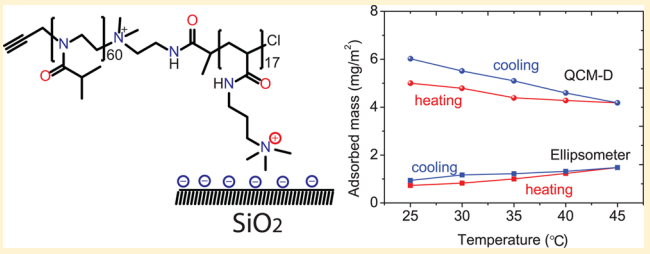

1. INTRODUCTION

Temperature-responsive surfaces have become increasingly important for the development of smart devices, particularly for biomedical applications, including drug delivery[1] and cell sheet engineering.[2] Such surfaces recognize a small change in the temperature of their environment and convert this signal into a macroscopic effect, such as a change in wettability, adhesion, and so forth. In most cases, this temperature sensitivity reflects conformational changes of thermosensitive polymer chains attached to the surface. Surfaces bearing poly(*N*-substituted-acrylamide) chains have been widely investigated, focusing primarily on poly(*N*-isopropylacrylamide) (PNIPAM).[3,4] Temperature-responsive surfaces based on oligo(ethylene glycol)methacrylates[5] and ethylene oxide-*co*-propylene oxide copolymers[6] have been explored as well, with particular focus on their nonfouling characteristics that are useful in biomedical applications. Poly(2-alkyl-2-oxazolines), where the alkyl group is methyl, ethyl, or isopropyl, also possess nonfouling properties,[7] yet there are only a few studies on their properties on surfaces. Poly(2-alkyl-2-oxazolines)-modified surfaces have mostly been obtained by the "grafting-on" method, which leads to the formation of polymer brushes.[8−11]

Recently, the "grafting-to" method has been employed to prepare poly(2-isopropyl-2-oxazoline) (PIPOZ) films onto a silicon substrate pretreated with a poly(glycidyl methacrylate) anchoring layer.[12] In this case, the grafted PIPOZ chains were linked to the substrate by multiple points of attachment, leading to formation of both loops and tails. The PIPOZ-grafted surfaces were used to immobilize gold nanoparticles, illustrating possible biomedical applications.

Studies of surface attached PIPOZ layers can also address fundamental questions. For instance, since the monomer unit of PIPOZ is a structural isomer of the repeat unit of PNIPAM, a comparative study of surfaces bearing PIPOZ or PNIPAM layers provides insights on the importance of the structural features inherent to a specific polymer in directing the overall properties of anchored polymer layers. Aqueous solutions of PIPOZ and PNIPAM exhibit a phase transition at a

Received: January 27, 2014
Revised: March 24, 2014
Published: April 2, 2014

   dx.doi.org/10.1021/la500377w | *Langmuir* 2014, 30, 4333−4341

temperature (T_c) in the ~30 to ~40 °C range, depending on polymer molecular weight and solution concentration.[13,14] Above this phase transition temperature, water becomes a poor solvent for the polymer chains and phase separation into a polymer-rich and a polymer-depleted phase occurs. Dehydrated PNIPAM chains undergo a coil-to-globule transition, followed by the aggregation of globules into larger mesoglobules ~ 200 nm in size.[15,16] The fate of PIPOZ chains upon dehydration is different. They undergo a conformational change and adopt a mostly all-trans conformation identical to the conformation the chains adopt in the polymer bulk,[17] as reported by Litt et al. in their description of the semicrystalline properties of PIPOZ.[18] The crystallization of PIPOZ also occurs in aqueous polymer solutions kept for several hours at temperatures exceeding the phase separation temperature, T_c.[19] It has been explained as being due to favorable dipolar interactions between the amide dipoles and nonspecific hydrophobic interactions between the isopropyl moieties. The study reported here was designed to monitor the temperature-dependent properties of electrostatically anchored PIPOZ layers on silica substrates.

The PIPOZ layers were prepared by adsorption of a diblock copolymer (PIPOZ$_{60}$-*b*-PAMPTMA$_{17}$) containing a PIPOZ block and a cationic block onto a negatively charged silica substrate. The composition of the copolymer was chosen to be similar to that of a copolymer of NIPAM (PNIPAM$_{48}$-*b*-PAMPTMA$_{20}$) used in previous studies.[20,21] We report here a study by ellipsometry and quartz crystal microbalance with dissipation (QCM-D) of PIPOZ copolymer layers formed under various conditions of pH and temperature. Data obtained from the two techniques yield the adsorbed polymer mass as well as the thickness and water-content of the polymer layer for temperatures between 25 and 45 °C. Significant adsorption hysteresis is observed during heating−cooling cycles.

2. MATERIALS AND METHODS

2.1. Materials. Poly(2-isopropyl-2-oxazoline)$_{60}$-*b*-poly((3-acrylamidopropyl)trimethylammonium)$_{17}$, abbreviated as (PIPOZ$_{60}$-*b*-PAMPTMA$_{17}$), was prepared as described previously with a molecular weight M_n of 10.3 kDa (Figure 1).[22] The nonionic block, PIPOZ, has a M_n of 7.0 kDa with M_w/M_n = 1.06 as determined by GPC,[31] corresponding to ~60 repeat units. This polymer was used here in control experiments aimed at evaluating the adsorption of PIPOZ on silica surfaces. The cationic block, PAMPTMA, contains one charge per repeat unit. The number of charged units per copolymer (~17) was determined by ^{1}H NMR spectroscopy.[22] The size and size distribution of the diblock copolymer could not be determined by GPC due to irreversible adsorption of the copolymer on the GPC packing material.[31] Sodium chloride (NaCl, BioXtra, ≥99.5%) was purchased from Sigma-Aldrich and used as received. All water used was first pretreated with a Milli-RO 10 plus unit and further purified with a Milli-Q PLUS 185 system. The resistivity after the treatment was 18.2 mΩ cm, and the total organic carbon content of the water did not exceed 2 ppb. The pH of the solutions was measured with a pH meter (PHM 210, Meterlab) and adjusted by adding small amounts of HCl (0.6 M) or NaOH (1 M) solutions.

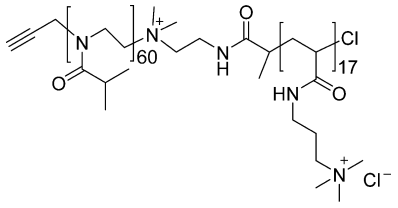

Figure 1. Chemical structure of poly(2-isopropyl-2-oxazoline)$_{60}$-*b*-poly((3-acrylamidopropyl)trimethylammonium)$_{17}$, abbreviated as PIPOZ$_{60}$-*b*-PAMPTMA$_{17}$.

QSX 303 silica sensors (Q-sense, Västra Frölunda, Sweden) were used in all QCM-D measurements. Silicon wafers coated with a 33 nm silica layer (Wafer net, Germany) were used in ellipsometry measurements. The cleaning procedures for silica sensors and silicon wafers can be found in the Supporting Information.

2.2. Ellipsometry. Ellipsometry is an optical technique that allows determination of thickness and refractive index of thin layers from changes in light polarization upon reflection.[23] In this work, a thin film ellipsometer, type 43603-200E (Rudolph Research with modification by Lund University, Sweden) was employed in null ellipsometry mode. A thorough description of the instrumental set up is provided elsewhere.[24] A xenon arc lamp with a filtered wavelength of 401.5 nm was used as the light source, and the angle of incidence was set to 67.5°. The Drude equation[25] was applied to determine the thickness (d) and refractive index (n) of the substrate and the adsorbed layer. The errors in the determination of d and n are covariant, meaning that the product of these two quantities, the surface excess (Γ), is subject to less uncertainty than these two quantities themselves. Γ was calculated using the de Feijter equation:[26]

$$\Gamma = d_l \frac{n_l - n_b}{\frac{dn}{dc}} \quad (1)$$

where subscripts "l" and "b" stand for adsorbed layer and bulk solution, respectively. A refractive index increment, dn/dc, of 0.1571 mL/g (measured at a wavelength of 450 nm in 0.1 mM NaCl solution by an Optilab DSP refractometer (Wyatt)) for PIPOZ$_{60}$-*b*-PAMPTMA$_{17}$ was used. The experimental procedure can be found in the Supporting Information, but we note already here that the refractive index increment is insensitive to temperature.[22]

2.3. Quartz Crystal Microbalance with Dissipation, QCM-D. QCM-D measurements enable determination of the mass of an adsorbed layer, including the associated solvent, by continuously measuring the change in frequency and dissipation at the fundamental frequency as well as at six overtone frequencies (15, 25, 35, 45, 55, 65 MHz). The frequency change observed during adsorption (Δf) depends on the total mass added to the crystal, including solvent coupled to the adsorbed layer. The change in energy dissipation (ΔD), that is, the energy loss caused by the adsorbed film, can provide insights regarding structural properties of adsorbed layers. A Q-sense E4 microbalance (Q-sense, Gothenburg) was employed in this study. A detailed description of the principal of operation has been published by Rodahl et al.[27]

For sufficiently thin, rigid and firmly anchored layers the sensed mass, m, can be determined according to the Sauerbrey equation:[28]

$$m = -C\frac{\Delta f}{n} \quad (2)$$

where C = 0.177 mg/m^2 for our sensors and n is the overtone number of the oscillation. The Sauerbrey equation has been suggested to be a good approximation when the change in dissipation is less than 2 × 10^{-6} per 5 Hz of Δf.[29]

The properties of the layer can be extracted using, for example, the Voigt model,[28] which is applicable when the energy dissipation is significant. Johannsmann et al. proposed an alternative viscoelastic model where the quartz resonator is modeled as an equivalent electrical circuit.[30] The Voigt model (including QCM-D experiments executed at different temperatures) and the Johannsman model are described in detail in the Supporting Information.

The mass obtained from these three models is the total mass oscillating with the crystal, that is, adsorbed polymer as well as coupled solvent. The mass fraction of water, X_w, and the effective hydrodynamic thickness, d_{eff},[31] can be evaluated by combining the surface excess, Γ, measured by ellipsometry and the mass, m, determined by QCM-D as

dx.doi.org/10.1021/la500377w | Langmuir 2014, 30, 4333−4341

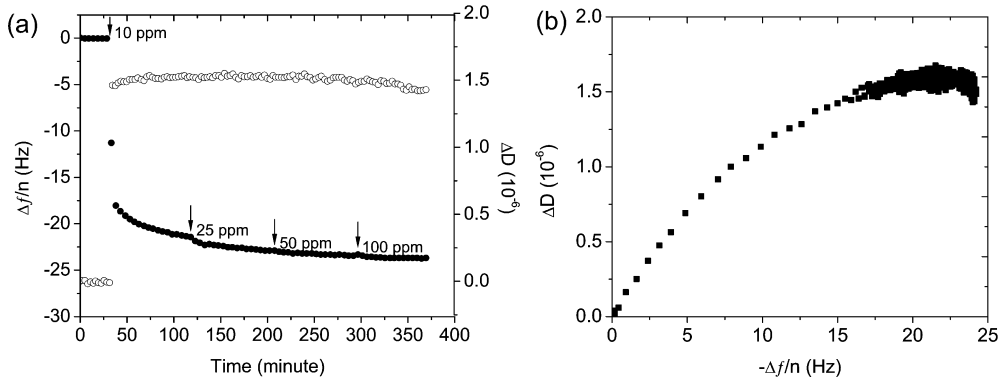

Figure 2. (a) Frequency (filled circles) and dissipation (open circles) change (data from the 7th overtone) versus time during adsorption of $PIPOZ_{60}$-*b*-$PAMPTMA_{17}$ to silica from solutions of increasing polymer concentration in 0.1 mM NaCl solution at pH 9, 25 °C. (b) The same data shown in a $\Delta D-\Delta f$ plot.

$$X_w = \frac{m - \Gamma}{m} \tag{3}$$

$$d_{eff} = \frac{m}{\rho_{eff}} = \frac{m}{\rho_p\left(\frac{\Gamma}{m}\right) + \rho_w X_w} \tag{4}$$

where ρ_{eff} is the effective density of the layer and the subscripts w and p stand for water and polymer, respectively. The value used for ρ_p is 1226 g/L.[32]

We mainly present QCM-D results obtained from Voigt modeling, but in some cases we also compare with results obtained from the Sauerbrey and Johannsmann models.

3. RESULTS

The effects of polymer concentration, pH, and temperature on the adsorption of $PIPOZ_{60}$-*b*-$PAMPTMA_{17}$ to silica are reported in this section. First, we discuss how the adsorbed layer of $PIPOZ_{60}$-*b*-$PAMPTMA_{17}$ is affected by the polymer concentration. Next, the pH effect on the adsorption of $PIPOZ_{60}$-*b*-$PAMPTMA_{17}$ to silica is demonstrated, and then we elucidate how the adsorbed mass varies due to temperature changes. We note that the aqueous diblock copolymer solution phase separates at a temperature of 46.1 °C.[22]

3.1. Concentration Effects on Adsorption. Adsorption of $PIPOZ_{60}$-*b*-$PAMPTMA_{17}$ to the QCM silica sensor results in a decrease in resonance frequency and an increase in energy dissipation, as demonstrated in Figure 2a for solutions (pH 9.0) ranging in concentration from 10 to 100 ppm (0.01 to 0.1 mg/mL). The changes in frequency and dissipation due to injection of the 10 ppm polymer solution are fast initially. However, slow changes occur over prolonged time, and full equilibrium has not been reached even after more than 1 h of adsorption. Increasing the polymer concentration to first 25 ppm and then 50 ppm leads to additional adsorption. We note that adsorption equilibrium is established at 50 ppm, as judged from no further changes in Δf and ΔD, and a further increase in polymer concentration to 100 ppm leads to marginally higher adsorption (see Figure 2). This suggests that the plateau in the adsorption isotherm is reached at about 50 ppm, and in the following QCM-D and ellipsometry experiments a concentration of 100 ppm was used to reach maximum adsorption. The magnitude of the dissipation change is small, indicating formation of a relatively thin adsorbed polymer layer on the sensor surface.

The $\Delta D-\Delta f$ plot, corresponding to the stepwise adsorption experiment (Figure 2a), is shown in Figure 2b. This type of plot can shed light on structural transitions occurring as the adsorbed layer develops, and in our case three stages can be distinguished. In the very early stage of adsorption, the dissipation increases close to linearly with frequency. This region ends at a frequency change of about 5 Hz. In the frequency range between 5 and 20 Hz, the slope of the ΔD versus Δf curve decreases. This decrease in the energy dissipated per unit sensed mass suggests stiffening of the layer due to increased interactions between adsorbed polymer chains. At the late stage of the adsorption process, corresponding to frequency changes between 20 and 25 Hz, the dissipation remains constant or even decreases somewhat due to further stiffening of the layer. This conclusion is supported by the Voigt modeling results that demonstrate that the shear viscosity and shear elasticity of the layer increase as the adsorption proceeds (see Figure S1 in the Supporting Information).

The sensed mass, including associated water, was estimated using three different models, and the results are provided in Figure 3. Clearly, the evaluated sensed mass depends on the

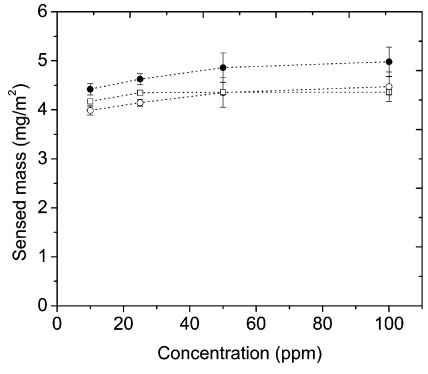

Figure 3. Sensed mass calculated using the Sauerbrey model (open circles), the Voigt model (filled circles), and the Johannsmann model (open squares), as a function of concentration at pH 9. The adsorption time was around 80 min at each concentration. Error bars were calculated based on three experiments.

model used, varying from 4.1 mg/m^2 (Sauerbrey model) to 4.9 mg/m^2 (Voigt model, the modeling parameters are available in Table S1 in the Supporting Information) at 100 ppm. This suggests that the Sauerbrey model underestimates the mass when applied to a layer with a dissipation change larger than 1×10^{-6}, which is consistent with other published data. Another feature that can be seen from Figure 3 is that the sensed mass

dx.doi.org/10.1021/la500377w | Langmuir 2014, 30, 4333−4341

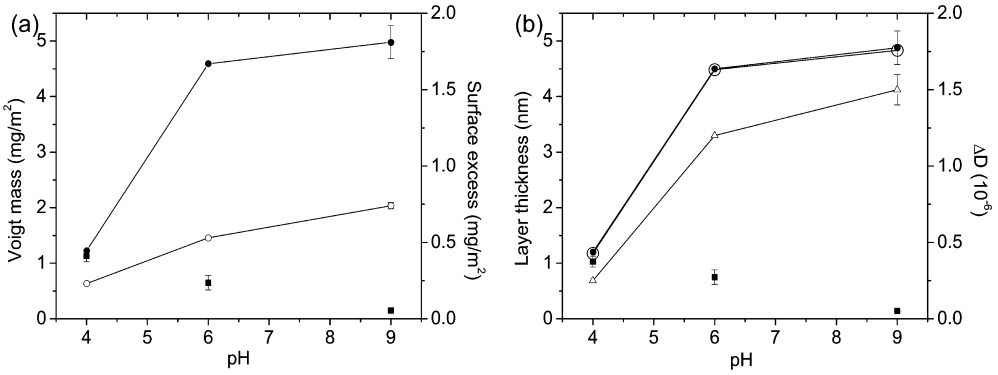

Figure 4. (a) Voigt mass (filled circles) and surface excess (open circles) of PIPOZ$_{60}$-*b*-PAMPTMA$_{17}$ and Voigt mass (filled squares) of PIPOZ$_{60}$ as a function of pH measured at 25 °C. (b) Layer thickness obtained by Voigt modeling (filled circles) and by eq 4 (open circles), as well as dissipation change (open triangles) of PIPOZ$_{60}$-*b*-PAMPTMA$_{17}$ and Voigt thickness of PIPOZ$_{60}$ (filled squares) at different pH values. The polymer concentration was in all cases 100 ppm.

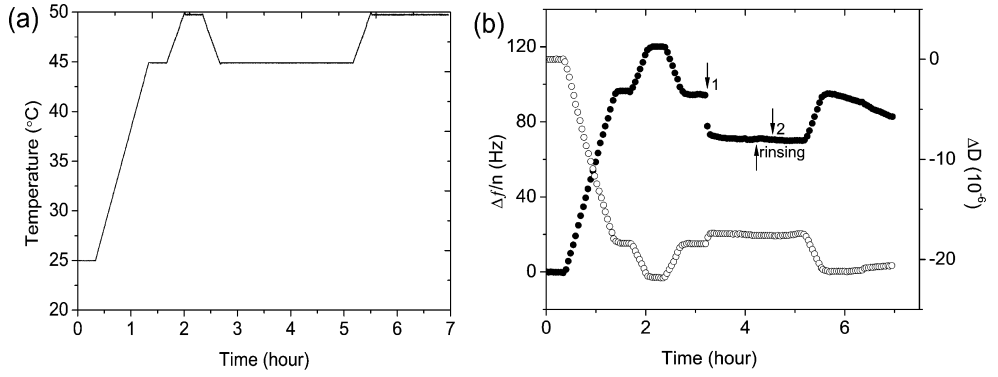

Figure 5. (a) Temperature versus time profile corresponding to the data shown in panel (b). (b) Δf (filled circles) and ΔD (open circles) as a function of time. 100 ppm PIPOZ$_{60}$-*b*-PAMPTAM$_{17}$ solution at pH 9 was injected at arrows 1 and 2. We note that the temperature was increased to 50 °C after 5.7 h, which results in a continuous change in frequency and dissipation due to precipitation of the block copolymer.

increases only slightly with increasing concentration. This reflects the high affinity of the cationic block to the negatively charged surface. Since equilibrium was approached very slowly at the lower concentrations, we suggest that the adsorption isotherm is even flatter than indicated in Figure 3.

3.2. pH Effects on Adsorption. Adsorption of PIPOZ$_{60}$-*b*-PAMPTAM$_{17}$ to silica from 100 ppm polymer solution in 0.1 mM NaCl at pH 4, 6, and 9 was investigated by both QCM-D and ellipsometry. As shown in Figure 4a, both the Voigt mass and the surface excess increase with increasing pH. This is due to the increased negative surface charge density of silica at elevated pH,[33] which means that a higher amount of the cationic PAMPTMA block can adsorb to the surface before neutralization is achieved. Indeed, for other cationic-nonionic block copolymers, it has been shown that the adsorption in the plateau region is dictated by electrostatic forces as long as the steric repulsion between the nonionic chains is not too large.[21] In order to determine if the PIPOZ$_{60}$ block also has affinity to the silica surface, QCM-D experiments were performed using a concentration of 100 ppm of this block. As shown in Figure 4a, the homopolymer of PIPOZ adsorbs to the silica surface, but significantly less than the diblock copolymer at pH 6 and pH 9. Further, while the adsorption of the diblock copolymer increases with increasing pH that of PIPOZ$_{60}$ decreases. This means that the two blocks are more segregated in the adsorbed layer at higher pH, with the cationic block accumulated at the surface and the PIPOZ block extending further toward the solution side, an effect that has been theoretically demonstrated using mean-field lattice theory.[21]

By comparing the ellipsometry and QCM-D data we note that the Voigt mass for PIPOZ$_{60}$-*b*-PAMPTMA$_{17}$ is, at all measured pH values, significantly larger than the surface excess at the corresponding pH. This reflects the high water content in the layer, which, by applying eq 3, is estimated to be 81% at pH 4, 88% at pH 6, and 85% at pH 9.

The layer thickness extracted from Voigt modeling and the effective thickness d_{eff} calculated from eq 4 are compared in Figure 4b. The two curves overlap well, demonstrating good consistency. The thickness of the adsorbed polymer layer increases from 1.2 nm at pH 4 to about 5 nm at pH 9, revealing that the polymer layer adopts a more extended conformation at higher surface coverage, which also gives rise to increased dissipation. We note that the Voigt thickness is an average value that should be used with care when the surface coverage is low. For instance, the thickness of the PIPOZ$_{60}$ layer is below 1 nm both at pH 9 and pH 6, which reflects the low surface coverage and not necessarily the extension of the PIPOZ chain normal to the surface. The same argument holds for all data obtained at pH 4.

3.3. Temperature Effects on Adsorption. *3.3.1. Polymer Deposition above the Phase Transition Temperature.* PIPOZ$_{60}$-*b*-PAMPTAM$_{17}$ is highly soluble in water at room temperature. However, aqueous PIPOZ$_{60}$-*b*-PAMPTAM$_{17}$ solutions become opaque when heated above 40 °C (corresponding to the onset of the endothermic peak in DSC

dx.doi.org/10.1021/la500377w | *Langmuir* 2014, 30, 4333−4341

measurements), signaling that water becomes a poor solvent for the PIPOZ block and the phase transition temperature (T_c) determined by differential scanning microcalorimetry is 46.1 °C (maximum of the endothermic peak).[22] In order to determine how the phase separation occurring in bulk solution affects events at the silica/water interface, a QCM-D experiment was performed while heating the solution up to 50 °C. The temperature−time profile together with the corresponding frequency and dissipation changes are presented in Figure 5.

Data were first recorded upon heating a 0.1 mM NaCl solution at pH 9 within the QCM sample cell to establish the baseline at different temperatures. Next, a 100 ppm polymer solution was injected at 45 °C, and adsorption was monitored for 50 min. Subsequently, the cell was rinsed with an aqueous 0.1 mM NaCl solution prior to injection of a fresh polymer solution (100 ppm). The rinsing and readdition of polymer hardly affected the frequency and dissipation values, indicating that equilibrium was reached. Subsequently, the temperature was increased to 50 °C without flushing away the excess polymer in the cell. The change in frequency and dissipation observed during this heating stage may be due to both changes in the sensor response and adsorption, and thus we do not discuss these further. However, once a temperature of 50 °C was established any change in frequency and dissipation is due to changes in the polymer layer. We find a continuous decrease in frequency and increase in dissipation, revealing that polymer aggregates precipitated on top of the polymer layer formed at 45 °C. Thus, bulk phase separation leads to deposition, as also concluded for hydroxypropylmethylcellulose solutions at high temperatures.[34] We conclude that aggregate deposition occurs above T_c, but below this value a monolayer of PIPOZ$_{60}$-*b*-PAMPTAM$_{17}$ adsorbs to the surface. In the remainder of this report we focus on layers formed below T_c.

3.3.2. Temperature-Dependence of Adsorption below the Phase Transition Temperature. Adsorption of PIPOZ$_{60}$-*b*-PAMPTAM$_{17}$ at different temperatures was investigated by ellipsometry, and the data are summarized in Figure 6. The surface excess was first determined at 25 °C and then the solution was heated and the surface excess was determined again after equilibration at elevated temperatures (the detailed experimental procedure is described in the Supporting Information). We find that adsorption increases significantly with increasing temperature, from 0.73 ± 0.02 mg/m^2 at 25 °C to 1.5 mg/m^2 at 45 °C. In the subsequent cooling process, the surface excess decreases again, but surface excess data obtained on heating and cooling do not coincide. Thus, a fraction of the polymer chains that adsorbed on the surface upon heating did not desorb on cooling, at least within the time scale of the experiment (approximately 4 h in total).

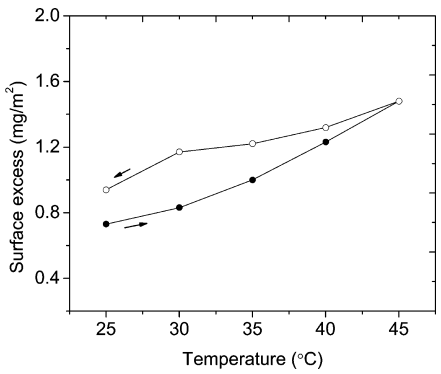

Figure 6. Surface excess of PIPOZ$_{60}$-*b*-PAMPTAM$_{17}$ on silica as a function of temperature. Adsorption occurred from 100 ppm polymer solution in 0.1 mM NaCl at pH 9. The arrows indicate the direction of the temperature change. Filled circles and open circles represent data obtained during the heating and the cooling stage, respectively.

Adsorption of PIPOZ$_{60}$-*b*-PAMPTAM$_{17}$ at different temperatures was also investigated with QCM-D (the original data are available in Figure S3, Supporting Information), and the results are shown in Figure 7. We note that during the first heating process from 25 to 45 °C, the magnitudes of both Δf and ΔD decrease with increasing temperature (Figure 7a and b), and also the Voigt mass decreases due to heating (Figure 7c). Since the ellipsometry data show that the adsorbed mass increases with temperature, the decrease in mass sensed by the QCM-D crystal must arise from a decrease of the water content of the adsorbed layer at elevated temperatures. This is a consequence of the release of water molecules hydrodynamically trapped between adsorbed polymer chains as well as water bound to the polymer chains to bulk solvent. The decrease in Voigt mass occurs continuously from 25 to 45 °C prior to the macroscopic phase separation of PIPOZ$_{60}$-*b*-PAMPTAM$_{17}$ in water, which occurs at slightly higher temperature and results in precipitation (see Figure 5). The lower ΔD at higher temperature is ascribed to the formation of a more rigid layer as water is expelled.

During subsequent cooling from 45 to 25 °C, the magnitudes of Δf, ΔD and the Voigt mass increased again due to reincorporation of water in the layer. However, consistent with the ellipsometry data, they do not recover their original values. For a given temperature the magnitude of Δf and the Voigt mass is higher whereas ΔD is lower at the cooling stage than at the heating stage. These trends indicate that as the PIPOZ layer was heated to 45 °C and cooled back to 25 °C, the (cold) adsorbed layer was more rigid and had a higher mass, compared to the values prior to heating. As seen in Figure 7, the discrepancies are significant. Interestingly, the data obtained while reheating the cooled layer back to 45 °C nearly coincide with those recorded during the first cooling process. (see Figure 7).

The Voigt thickness of the adsorbed polymer layer versus temperature is shown in Figure 7d. The thickness decreases slightly upon heating and increases on cooling, ranging from 4 to 6 nm.

4. DISCUSSION

4.1. The Effect of pH on Layer Structure at the Silica/Water Interface. Adsorption of diblock copolymers usually leads to formation of a segregated layer, where the block with high affinity to the surface, the anchor block, is enriched close to the surface whereas the other block, the buoy block, extends toward solution.[35] The degree of segregation depends on the surface affinity of the two blocks. Our data show that the PIPOZ$_{60}$ homopolymer adsorbs less to silica with increasing pH. Thus, the two blocks will be more extensively segregated at the interface at higher pH, approaching the classical situation with an adsorbing anchor block (the cationic PAMPTMA block) and a nonadsorbing buoy block (the PIPOZ block) that is tethered to the surface by the anchor.

The silica surface charge density increases with increasing pH, and as a result the surface excess of PIPOZ$_{60}$-*b*-PAMPTAM$_{17}$ increases (see Figure 4). This means that the PIPOZ chains will be anchored closer to each other, which will affect the conformation of the polymer chains due to mutual

dx.doi.org/10.1021/la500377w | Langmuir 2014, 30, 4333−4341

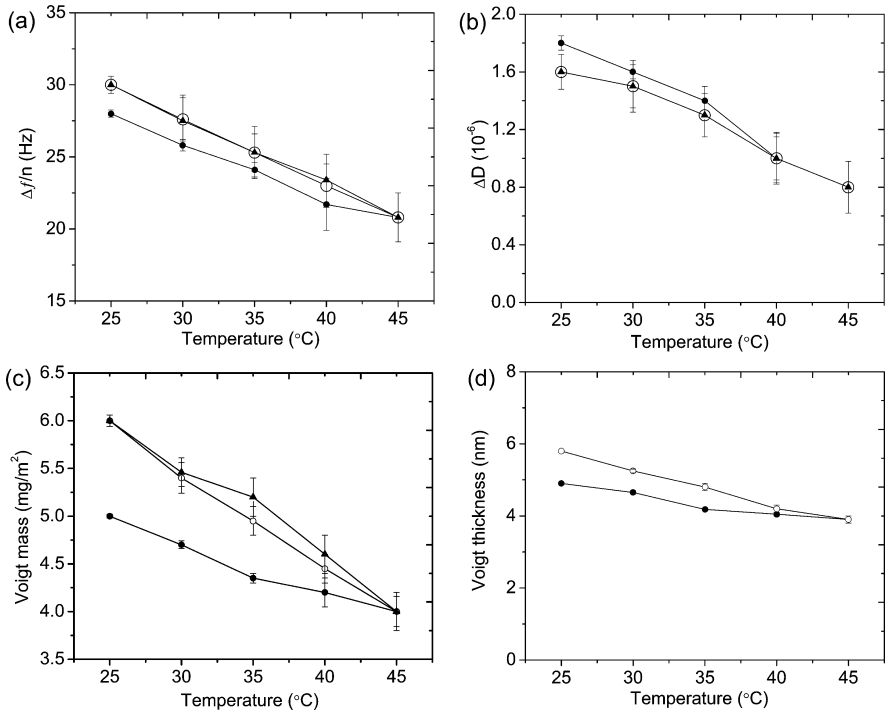

Figure 7. (a) Magnitude of the frequency change ($-\Delta f$) due to PIPOZ$_{60}$-*b*-PAMPTMA$_{17}$ adsorption to silica from 100 ppm 0.1 mM NaCl solution as a function of temperature at pH 9. (b) Corresponding dissipation change ΔD. (c) Voigt mass as a function of temperature. (d) Voigt thickness as a function of temperature. Filled circles and filled triangles represent data obtained during the first heating and the second heating stages, respectively, and open circles represent the first cooling stage.

interactions. Under good solvent conditions and sufficiently high surface densities, the polymer chains will stretch away from the surface to avoid overlapping, resulting in a brush-like conformation.[36] The degree of stretching can be estimated by comparing the Flory radius of the tethered chain and the average distance between the chains tethered to the surface. The Flory radius, R_F,[37] of a PIPOZ$_{60}$ chain can be estimated from eq 5:

$$R_F = ln^{\alpha} \tag{5}$$

where l is the contour length of the repeating unit that is 0.32 nm,[18,19] n is the degree of polymerization, and α is an exponent that depends on the solvent condition, with $\alpha = 0.5$ in a theta solvent and $\alpha \approx 0.6$ in a good solvent. This gives $R_F = 2.5-3.7$ nm, depending on solvent condition.

The spacing between the anchoring points, D, can be calculated from $D = \sigma^{-0.5}$, where σ is the number of chains per unit surface area that can be determined from the surface excess.[38] The results are shown in Table 1. Under good solvent conditions (i.e., low temperatures) at pH 4, the distance between anchoring points is larger than $2R_F$, and the overlap between chains is thus minor. At pH 6 and pH 9 D is somewhat lower than $2R_F$ and the polymer chains start to overlap and the PIPOZ chains will be slightly stretched away from the surface.

The layer thickness is determined by the polymer conformation and distance between anchoring points. When the grafting density is low as at pH 4, the polymer will lie relatively flat on the surface with a thickness that is around 1 nm in our case (Figure 4b). The higher grafting density at pH 9 leads to a more extended layer, and in our case the thickness reaches 5 nm at this pH.

Table 1. Surface Excess and Distance, *D*, between Adsorbed Polymer Chains at 25 °C

			$2R_F/D$	
pH	surface excess (mg/m^2)	D (nm)	good solvent	theta solvent
4	0.23	8.6	0.86	0.58
6	0.53	5.7	1.3	0.88
9	0.73	4.9	1.5	1.0

4.2. The Effect of Temperature on Adsorption and Layer Structure. It is generally expected that the adsorption of a polymer increases as the solvent quality decreases,[37] and this has been observed to occur at higher temperatures for a range of temperature-responsive polymers such as poly(ethylene oxide)[39] and NIPAM.[40] Thus, the increasing surface excess with increasing temperature obtained in this work for PIPOZ$_{60}$-*b*-PAMPTAM$_{17}$ is in line with expectations.

It is interesting to note the difference between the ellipsometry and the QCM-D results. The surface excess increases with increasing temperature (Figure 6), whereas the Voigt mass decreases with increasing temperature (Figure 7c). This reflects that the two techniques measure different quantities. From the ellipsometry measurements, we learn that PIPOZ$_{60}$-*b*-PAMPTAM$_{17}$ adsorbs more at higher temperatures due to the worsening of the solvent quality of water for the PIPOZ chain. From QCM-D, we learn that the mass of the polymer plus the amount of associated water decreases with increasing temperature. Thus, the water content of the layer decreases significantly due to the worsening of the solvent quality, and this effect is quantified in Figure 8. A gradual decrease in the water content of the adsorbed layer is observed on heating, and on cooling a gradual rehydration occurs. The slightly higher water content at a given temperature observed

dx.doi.org/10.1021/la500377w | *Langmuir* 2014, 30, 4333−4341

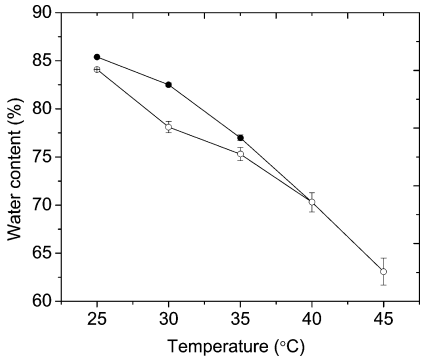

Figure 8. Water content of the $PIPOZ_{60}$-*b*-$PAMPTAM_{17}$ layer adsorbed on silica as a function of temperature at pH 9. Filled circles and open circles represent data obtained during the heating and the cooling stage, respectively.

on heating compared to on cooling is related to the adsorption hysteresis shown in Figures 6 and 7.

A common feature of many thermoresponsive polymers is a structure where polar and nonpolar chemical groups are located close to each other, rendering hydration particularly intriguing knowing that clathrate-like structures are preferred around nonpolar solutes whereas direct hydrogen bonds and favorable dipolar interactions exist between polar groups and water. The temperature responsive block that is in focus of this report, $PIPOZ_{60}$, has a phase transition temperature, T_c, of 46.1 °C.[22] However, the dehydration of the amide groups in the PIPOZ homopolymer occurs gradually from 20 °C,[17] which is also observed for adsorbed layers of $PIPOZ_{60}$-*b*-$PAMPTAM_{17}$ in our work (Figure 8). It has been reported that a water layer surrounds PIPOZ in cold water, but this water layer gradually disappears due to breakdown of carbonyl/water hydrogen bonds with increasing temperature.[17] The formation and loss of hydrogen bonds due to temperature variations in poly(2-isopropyl-2-oxazoline) brush layers prepared by the grafting-to method has been observed by ATR-FTIR, which was detected as a temperature-reversible upward shift of the adsorption band of the amide groups.[12] Another interesting feature is that the PIPOZ chains adopt mostly trans conformations above T_c, which facilitates interchain dipolar interactions between amide groups and possibly promotes partial organization of the chains.[17,19] The conformational change decreases the steric repulsion between the polymer chains and new favorable interactions may occur since the new conformation is reminiscent of the conformation of the chain in the crystal, and this is likely to facilitate increased polymer adsorption and further dehydration of the adsorbed layer. When the solvent condition becomes sufficiently poor, aggregation occurs in bulk solution[17] and polymer aggregates deposit on top of the adsorbed layer, as shown in Figure 5. Consistent with this, the adsorption of hydrophobically end-modified poly(2-isopropyl-2-oxazoline) at the air/water interface has been reported to be enhanced by a temperature increase, and as the temperature reaches T_c the PIPOZ chains interact and form aggregates that pack into a dense 2-D structure.[41]

The changes in ΔD upon heating also indicate that the structure of the adsorbed $PIPOZ_{60}$-*b*-$PAMPTAM_{17}$ polymer layer is altered by a temperature cycle. Upon heating, ΔD decreases (Figure 7), indicating that the layer becomes more compact as a result of dehydration and further adsorption. During the cooling process, ΔD increases again due to rehydration that causes some desorption and swelling of the layer. Importantly, ΔD does not increase to the same value as observed before heating. This is related to the adsorption hysteresis discussed in the following section.

4.3. Hysteresis Due to Temperature Cycling. PIPOZ is soluble in aqueous solutions at temperatures below the lower critical solution temperature (LCST), and it can readily recover its solubility upon cooling after dehydration above LCST for a short period of time.[17,42] However, the phase transition is not reversible if the PIPOZ solution is kept for hours above LCST, due to the formation of PIPOZ crystals that do not dissolve in cold water.[17,19] Long-lived temperature-induced self-association structures (formed in solution heated above LCST for 10 min, but remaining as the solution is cooled down) has also been noted for grafted PIPOZ chains on pullulan.[42]

In case equilibrium is established between the bulk and an adsorbed layer, fully reversible solution properties should give reversible adsorbed layer structures in a temperature cycle. However, in this work, we note a pronounced temperature hysteresis in the surface excess even below temperatures where hysteresis is found in bulk solutions of PIPOZ containing polymers. Thus, the presence of adsorption hysteresis shows that equilibrium between the bulk and the adsorbed layer is established very slowly, and trapped nonequilibrium states are formed. This can be understood by considering the desorption process, which can be regarded as proceeding in two steps. First, the molecule has to completely detach from the surface to reach the subsurface region just outside the adsorbed layer. Next, the molecules have to be transported away from the surface toward the bulk solution by diffusion driven by the concentration gradient. In order for the molecule to detach from the surface and reach the subsurface region, all binding sites have to be broken. The block copolymer $PIPOZ_{60}$-*b*-$PAMPTAM_{17}$ has 17 cationic groups which all can bind strongly to the negatively charged silica surface. That all these groups should detach at the same time and allow the molecule to reach the subsurface region is an unlikely event, and thus, this process is slow due to the high activation energy of desorption. The following transport from the subsurface region is also slow since the concentration gradient is small, particularly when the adsorption isotherm is of high-affinity type[43] as in our case (Figure 3).

Adsorption hysteresis is the main course of the temperature hysteresis found in our QCM-D and ellipsometry results. However, we note that a small hysteresis in the QCM-D response also has been noted for PNIPAM chains grafted to gold, and attributed to slow changes in hydration.[44] Thus, such effects may also play a role in our QCM-D experiments.

4.4. Water Content in the Layer. At room temperature, the water content of the adsorbed $PIPOZ_{60}$-*b*-$PAMPTMA_{17}$ layer on silica is found to be in the range of 81% to 88% depending on the pH-value. For layers of the structurally similar copolymer $PNIPAM_{48}$-*b*-$PAMPTMA_{20}$ on silica the water content was found to be around 87%,[20] which is close to that found for the $PIPOZ_{60}$-*b*-$PAMPTMA_{17}$ layer. However, a significantly higher water content, around 95%, was found for a cationic/nonionic diblock copolymer $(METAC)_m$-*b*-$(PEO_{45}MEMA)_n$ layer, where the nonionic block has a bottle-brush structure.[45] At a temperature close to T_c, the water content of the $PIPOZ_{60}$-*b*-$PAMPTMA_{17}$ layer is around 65%. This water content is due to both water trapped within the layer and water directly hydrating the polymer chain, and we note that Korchagina et al. reported that the PIPOZ chains

dx.doi.org/10.1021/la500377w | *Langmuir* 2014, 30, 4333−4341

of the diblock copolymer were not fully dehydrated even above the phase-transition temperature.[22]

5. CONCLUSIONS

Thermoresponsive polymer layers of $PIPOZ_{60}$-*b*-$PAMPTMA_{17}$ have been formed on silica surfaces through physisorption driven primarily by electrostatic interactions. The high affinity between the cationic block and the negatively charged silica resulted in marginally increased adsorbed mass with increasing concentration (10−100 ppm). The predominance of electrostatic interactions leads to higher surface excess at higher pH values. Since the affinity of PIPOZ to silica also decreases with increasing pH, the layer becomes more segregated with the PIPOZ chains being more extended toward solution. The decreasing solvency for the PIPOZ block with increasing temperature results in a pronounced increase in adsorbed mass, and above the bulk phase separation temperature aggregates are slowly depositing on the surface. The Voigt mass, which also includes the mass of water hydrodynamically coupled to the polymer layer, decreases upon heating due to expulsion of water from the layer. A clear hysteresis in layer properties was observed when the temperature was cycled between 25 and 45 °C. This provides evidence of the predominance of trapped states that are slow to relax toward the equilibrium state due to the many electrostatic binding sites between the cationic anchor block and the surface, and due to the slow diffusion away from the subsurface region that occurs due to the small concentration gradient.

■ ASSOCIATED CONTENT

Supporting Information

Voigt model, Johannsmann model, and temperature-dependent adsorption data obtained by QCM-D. This material is available free of charge via the Internet at http://pubs.acs.org.

■ AUTHOR INFORMATION

Corresponding Author

*E-mail: percl@kth.se.

Notes

The authors declare no competing financial interest.

■ ACKNOWLEDGMENTS

P.M.C. and J.A. acknowledge a grant from the Swedish Research Council, VR. A.D. acknowledges a VINNMER fellowship from VINNOVA. The work was supported in part by a grant of the Natural Sciences and Engineering Research Council of Canada to F.M.W.

■ REFERENCES

(1) Contreras-García, A.; Alvarez-Lorenzo, C.; Taboada, C.; Concheiro, A.; Bucio, E. Stimuli−Responsive Networks Grafted onto Polypropylene for the Sustained Delivery of Nsaids. *Acta Biomater.* **2011**, *7*, 996−1008.

(2) Akiyama, Y.; Kikuchi, A.; Yamato, M.; Okano, T. Ultrathin Poly(*N*-isopropylacrylamide) Grafted Layer on Polystyrene Surfaces for Cell Adhesion/Detachment Control. *Langmuir* **2004**, *20*, 5506−5511.

(3) Han, C.-C.; Wei, T.-C.; Wu, C.-S.; Liu, Y.-L. Temperature-Responsive Poly(Tetrafluoroethylene) Membranes Grafted with Branched Poly(*N*-isopropylacrylamide) Chains. *J. Membr. Sci.* **2010**, *358*, 60−66.

(4) Cooperstein, M. A.; Canavan, H. E. Biological Cell Detachment from Poly(N-isopropyl acrylamide) and Its Applications. *Langmuir* **2009**, *26*, 7695−7707.

(5) Raynor, J.; Capadona, J.; Collard, D.; Petrie, T.; García, A. Polymer Brushes and Self-Assembled Monolayers: Versatile Platforms to Control Cell Adhesion to Biomaterials (Review). *Biointerphases* **2009**, *4* (2), FA3−16.

(6) Malal, R.; Malal, M.; Cohn, D. Surface Grafting Thermoresponsive PEO−PPO−PEO Chains. *J. Tissue Eng. Regener. Med.* **2011**, *5*, 394−401.

(7) Konradi, R.; Acikgoz, C.; Textor, M. Polyoxazolines for Nonfouling Surface Coatings — A Direct Comparison to the Gold Standard PEG. *Macromol. Rapid Commun.* **2012**, *33*, 1663−1676.

(8) Jordan, R.; Ulman, A. Surface Initiated Living Cationic Polymerization of 2-Oxazolines. *J. Am. Chem. Soc.* **1998**, *120*, 243−247.

(9) Zhang, N.; Steenackers, M.; Luxenhofer, R.; Jordan, R. Bottle-Brush Brushes: Cylindrical Molecular Brushes of Poly(2-oxazoline) on Glassy Carbon. *Macromolecules* **2009**, *42*, 5345−5351.

(10) Rehfeldt, F.; Tanaka, M.; Pagnoni, L.; Jordan, R. Static and Dynamic Swelling of Grafted Poly(2-alkyl-2-oxazoline)s. *Langmuir* **2002**, *18*, 4908−4914.

(11) Konradi, R.; Pidhatika, B.; Muhlebach, A.; Textor, M. Poly-2-methyl-2-oxazoline: A Peptide-like Polymer for Protein-Repellent Surfaces. *Langmuir* **2008**, *24*, 613−616.

(12) Agrawal, M.; Rueda, J. C.; Uhlmann, P.; Müller, M.; Simon, F.; Stamm, M. Facile Approach to Grafting of Poly(2-oxazoline) Brushes on Macroscopic Surfaces and Applications Thereof. *ACS Appl. Mater. Interfaces* **2012**, *4*, 1357−1364.

(13) Schild, H. G. Poly(*N*-isopropylacrylamide): Experiment, Theory and Application. *Prog. Polym. Sci.* **1992**, *17*, 163−249.

(14) Diab, C.; Akiyama, Y.; Kataoka, K.; Winnik, F. M. Microcalorimetric Study of the Temperature-Induced Phase Separation in Aqueous Solutions of Poly(2-isopropyl-2-oxazolines). *Macromolecules* **2004**, *37*, 2556−2562.

(15) Wu, C.; Li, W.; Zhu, X. X. Viscoelastic Effect on the Formation of Mesoglobular Phase in Dilute Solutions. *Macromolecules* **2004**, *37*, 4989−4992.

(16) Kujawa, P.; Aseyev, V.; Tenhu, H.; Winnik, F. M. Temperature-Sensitive Properties of Poly(*N*-isopropylacrylamide) Mesoglobules Formed in Dilute Aqueous Solutions Heated above Their Demixing Point. *Macromolecules* **2006**, *39*, 7686−7693.

(17) Katsumoto, Y.; Tsuchiizu, A.; Qiu, X.; Winnik, F. M. Dissecting the Mechanism of the Heat-Induced Phase Separation and Crystallization of Poly(2-isopropyl-2-oxazoline) in Water through Vibrational Spectroscopy and Molecular Orbital Calculations. *Macromolecules* **2012**, *45*, 3531−3541.

(18) Litt, M.; Rahl, F.; Roldan, L. G. Polymerization of Cyclic Imino Ethers. VI. X-ray Study of Some Polyaziridines. *J. Polym. Sci., Part A-2* **1969**, *7*, 463−473.

(19) Demirel, A. L.; Meyer, M.; Schlaad, H. Formation of Polyamide Nanofibers by Directional Crystallization in Aqueous Solution. *Angew. Chem., Int. Ed.* **2007**, *46*, 8622−8624.

(20) Dedinaite, A.; Thormann, E.; Olanya, G.; Claesson, P. M.; Nystrom, B.; Kjoniksen, A.-L.; Zhu, K. Friction in Aqueous Media Tuned by Temperature-responsive Polymer Layers. *Soft Matter* **2010**, *6*, 2489−2498.

(21) Shovsky, A.; Knohl, S.; Dedinaite, A.; Zhu, K.; Kjøniksen, A.-L.; Nyström, B.; Linse, P.; Claesson, P. M. Cationic Poly(*N*-isopropylacrylamide) Block Copolymer Adsorption Investigated by Dual Polarization Interferometry and Lattice Mean-Field Theory. *Langmuir* **2012**, *28*, 14028−14038.

(22) Korchagina, E. V.; Qiu, X.-P.; Winnik, F. M. Effect of Heating Rate on the Pathway for Vesicle Formation in Salt-Free Aqueous Solutions of Thermosensitive Cationic Diblock Copolymers. *Macromolecules* **2013**, *46*, 2341−2351.

(23) Gonçalves, D.; Irene, E. A. Fundamentals and Applications of Spectroscopic Ellipsometry. *Quim. Nova* **2002**, *25*, 794−800.

(24) Landgren, M.; Joensson, B. Determination of The Optical Properties of Silicon/Silica Surfaces by Means of Ellipsometry, Using Different Ambient Media. *J. Phys. Chem.* **1993**, *97*, 1656−1660.
(25) Malmsten, M.; Lindman, B. Ellipsometry Studies of The Adsorption of Cellulose Ethers. *Langmuir* **1990**, *6*, 357−364.
(26) De Feijter, J. A.; Benjamins, J.; Veer, F. A. Ellipsometry as a Tool to Study The Adsorption Behavior of Synthetic and Biopolymers at The Air−Water Interface. *Biopolymers* **1978**, *17*, 1759−1772.
(27) Rodahl, M. H. F.; Krozer, A.; Brzezinski, P.; Kasemo, B. Quartz Crystal Microbalance Set Up for Frequency and Q-Factor Measurements in Gaseous and Liquids Environments. *Rev. Sci. Instrum.* **1995**, *66*, 3924−3930.
(28) Voinova, M. V. R. M.; Jonson, M.; Kasemo, B. Viscoelastic Acoustic Response of Layered Polymer Films at Fluid-Solid Interfaces: Continuum Mechanics Approach. *Phys. Scr.* **1999**, *59*, 391−396.
(29) Reviakine, I.; Johannsmann, D.; Richter, R. P. Hearing What You Cannot See and Visualizing What You Hear: Interpreting Quartz Crystal Microbalance Data from Solvated Interfaces. *Anal. Chem.* **2011**, *83*, 8838−8848.
(30) Johannsmann, D.; Grüner, J.; Wesser, J.; Mathauer, K.; Wegner, G.; Knoll, W. Visco-elastic Properties of Thin Films Probed with a Quartz Crystal Resonator. *Thin Solid Films* **1992**, *210−211* (Part 2), 662−665.
(31) Höök, F.; Kasemo, B.; Nylander, T.; Fant, C.; Sott, K.; Elwing, H. Variations in Coupled Water, Viscoelastic Properties, and Film Thickness of a Mefp-1 Protein Film during Adsorption and Cross-Linking: A Quartz Crystal Microbalance with Dissipation Monitoring, Ellipsometry, and Surface Plasmon Resonance Study. *Anal. Chem.* **2001**, *73*, 5796−5804.
(32) Diehl, C.; Cernoch, P.; Zenke, I.; Runge, H.; Pitschke, R.; Hartmann, J.; Tiersch, B.; Schlaad, H. Mechanistic Study of The Phase Separation/Crystallization Process of Poly(2-isopropyl-2-oxazoline) in Hot Water. *Soft Matter* **2010**, *6*, 3784−3788.
(33) Bolt, J. H. Determination of the Charge Density of Silica Sols. *J. Phys. Chem.* **1957**, *61*, 1166−1169.
(34) Bodvik, R.; Macakova, L.; Karlson, L.; Thormann, E.; Claesson, P. Temperature-Dependent Competition between Adsorption and Aggregation of a Cellulose Ether—Simultaneous Use of Optical and Acoustical Techniques for Investigating Surface Properties. *Langmuir* **2012**, *28*, 9515−9525.
(35) Marques, C.; Joanny, J. F.; Leibler, L. Adsorption of Block Copolymers in Selective Solvents. *Macromolecules* **1988**, *21*, 1051−1059.
(36) Zhao, B.; Brittain, W. J. Polymer Brushes: Surface-Immobilized Macromolecules. *Prog. Polym. Sci.* **2000**, *25*, 677−710.
(37) Fleer, G. J.; Stuart, M. A. C.; Scheutjens, J. M. H. M.; Cosgrove, T.; Vincent, B. *Polymers at interfaces*; Chapman & Hall: London, 1993; pp 265−271.
(38) Milner, S. T.; Witten, T. A.; Cates, M. E. Theory of the Grafted Polymer Brush. *Macromolecules* **1988**, *21*, 2610−2619.
(39) Claesson, P. M.; Gölander, C.-G. Direct Measurements of Steric Interactions between Mica Surfaces Covered with Electrostatically Bound Low-Molecular-Weight Polyethylene Oxide. *J. Colloid Interface Sci.* **1987**, *117*, 366−374.
(40) Tanahashi, T.; Kawaguchi, M.; Honda, T.; Takahashi, A. Adsorption of Poly(*N*-isopropylacrylamide) on Silica Surfaces. *Macromolecules* **1994**, *27*, 606−607.
(41) Obeid, R.; Park, J.-Y.; Advincula, R. C.; Winnik, F. M. Temperature-Dependent Interfacial Properties of Hydrophobically End-Modified Poly(2-isopropyl-2-oxazoline)s Assemblies at the Air/Water Interface and on Solid Substrates. *J. Colloid Interface Sci.* **2009**, *340*, 142−152.
(42) Morimoto, N.; Obeid, R.; Yamane, S.; Winnik, F. M.; Akiyoshi, K. Composite Nanomaterials by Self-Assembly and Controlled Crystallization of Poly(2-isopropyl-2-oxazoline)-Grafted Polysaccharides. *Soft Matter* **2009**, *5*, 1597−1600.
(43) Stuart, M. A. C.; Fleer, G. J. Adsorbed Polymer Layers in Nonequilibrium Situations. *Annu. Rev. Mater. Sci.* **1996**, *26*, 463−500.
(44) Zhang, G. Study on Conformation Change of Thermally Sensitive Linear Grafted Poly(*N*-isopropylacrylamide) Chains by Quartz Crystal Microbalance. *Macromolecules* **2004**, *37*, 6553−6557.
(45) Liu, X.; Dedinaite, A.; Rutland, M.; Thormann, E.; Visnevskij, C.; Makuska, R.; Claesson, P. M. Electrostatically Anchored Branched Brush Layers. *Langmuir* **2012**, *28*, 15537−15547.